Inorg. Chem. **2004**, *43*, 8510–8519

DNA Binding and Photocleavage in Vitro by New Dirhodium(II) dppz Complexes: Correlation to Cytotoxicity and Photocytotoxicity

Alfredo M. Angeles-Boza,[†] Patricia M. Bradley,[‡] Patty K.-L. Fu,[§] Sara E. Wicke,[‡] John Bacsa,[†] Kim R. Dunbar,*[,†] and Claudia Turro*[,‡]

Department of Chemistry, The Ohio State University, Columbus, Ohio 43210, Department of Chemistry, Texas A&M University, College Station, Texas 77843, and Food and Drug Administration, 5100 Paint Branch Pkwy, College Park, Maryland 20740

Received July 9, 2004

Two new dirhodium(II) complexes possessing the intercalating dppz ligand (dppz = dipyrido[3,2-*a*:2′,3′-*c*]phenazine), *cis*-$[Rh_2(\mu\text{-}O_2CCH_3)_2(dppz)(\eta^1\text{-}O_2CCH_3)(CH_3OH)]^+$ (**1**) and *cis*-$[Rh_2(\mu\text{-}O_2CCH_3)_2(dppz)_2]^{2+}$ (**2**), were synthesized and characterized as potential agents for photochemotherapy. Various techniques show that **1** binds to DNA through intercalation, although some aggregation of the complex on the DNA surface is also present. In contrast, **2** does not intercalate between the DNA bases; however, strong hypochromic behavior is observed in the presence of DNA, which can be attributed to intermolecular π-stacking of **2** enhanced by the polyanion. The apparent DNA binding constants determined using optical titrations are compared to those from dialysis experiments. Both complexes photocleave pUC18 plasmid in vitro under irradiation with visible light ($\lambda_{irr} \geq 395$ nm, 15 min), resulting in the nicked, circular form. Greater photocleavage is observed for **1** relative to **2**, which may be due to the ability of **1** to intercalate between the DNA bases. The cytotoxicity toward human skin cells (Hs-27) measured as the concentration at which 50% cell death is recorded, LC_{50}, was found to be 135 ± 8 μM for **2** in the dark (30 min), which is significantly lower than those of **1** ($LC_{50} = 27 \pm 2$ μM) and $Rh_2(O_2CCH_3)_4$ ($LC_{50} = 15 \pm 2$ μM). Irradiation of cell cultures containing **1** and $Rh_2(O_2CCH_3)_4$ with visible light (400–700 nm, 30 min) has little effect on their cytotoxicity, with LC_{50} values of 21 ± 3 and 13 ± 2 μM, respectively. Interestingly, a 3.4-fold increase in the toxicity of **2** is observed when the cell cultures are irradiated (400–700 nm, 30 min), resulting in $LC_{50} = 39 \pm 1$ μM. The greater toxicity of **1** compared to **2** in the dark may be related to the ability of the former compound to intercalate between the DNA bases. The lower cytotoxicity of **2**, together with its significantly greater photocytotoxicity, makes this complex a potential agent for photodynamic therapy (PDT). These results suggest that intercalation or strong DNA binding may not be a desirable property of a potential PDT agent.

Introduction

The success of cisplatin (*cis*-$Pt(NH_3)_2Cl_2$) as an antitumor agent and the emerging practical uses of photodynamic therapy have led to the exploration of various new transition metal complexes for potential use in photochemotherapy.[1−6] Crucial challenges involving the use of cisplatin include its effectiveness toward some cancers and not others and the resistance developed by tumor cells to the drug.[5−9] The toxicity of cisplatin and other antitumor drugs toward healthy cells is also a concern.[5−9] Activation of otherwise nontoxic drugs through irradiation of tumors with visible or near-IR light provides a means to localize the action of the agent to the affected area, a field generally known as photodynamic

* Authors to whom correspondence should be addressed. E-mail: turro@chemistry.ohio-state.edu (C.T.); dunbar@mail.chem.tamu.edu (K.R.D.).
[†] Texas A&M University.
[‡] The Ohio State University.
[§] Food and Drug Administration.

(1) Evstigneeva, R. P.; Zitsev, A. V.; Luzgina, V. N. Ol'shevskaya, V. A. Shtil, A. A. *Curr. Med. Chem.: Anti-Cancer Agents* **2003**, *3*, 383.
(2) Tolomeo, M.; Simoni, D. *Curr. Med. Chem.: Anti-Cancer Agents* **2002**, *2*, 387.
(3) (a) Kanzaki, A.; Takebayashi, Y.; Ren, X.-Q.; Miyashita, H.; Mori, S.; Akiyama, S.-I.; Pommier, Y. *Mol. Cancer Ther.* **2002**, *1*, 1327. (b) Sodet, O.; Khan, Q. A.; Kohn, K. W.; Pommier, Y. *Curr. Med. Chem: Anti-Cancer Agents* **2003**, *3*, 271.
(4) Goldie, J. H. *Cancer Metastasis Rev.* **2001**, *20*, 63.
(5) Schoendorf, T.; Neumann, R.; Benz, C.; Becker, M.; Riffelmann, M.; Goehring, U.-J.; Sartorius, J.; von Koenig, C.-H. W.; Breidenbach, M.; Valter, M. M.; Hoopmann, M.; Di Nicolantonio, F.; Kurbacher, C. M. *Recent Results Cancer Res.* **2003**, *161*, 111.
(6) Broxterman, H. J.; Georgopapadakou, N. *Drug Resist. Updates* **2001**, *4*, 197.

10.1021/ic049091h CCC: $27.50
Published on Web 11/18/2004

therapy (PDT).[10−14] Many compounds are currently being investigated for potential use in PDT and are typically based on derivatives of porphyrins and phthalocyanins.[10−15] The photoactive drug Photofrin is in use for the photodynamic treatment of lung and esophageal cancers, and it is composed of a mixture of hematoporphyrin and its derivatives.[10−15] Typically, $^1O_2$ produced through energy transfer from the drug's long-lived $^3\pi\pi^*$ excited state is the reactive species that results in damage to biomolecules.[10] Drawbacks of current PDT agents are their prolonged cutaneous sensitivity and the requirement of O_2 for their function, since once consumed, O_2 must diffuse to the proximity of the agent.[10−15] In addition, some of the most malignant and drug resistant cancer cells are hypoxic.[16−18] New classes of transition metal PDT agents may prove to be useful in circumventing the problems associated with the current drugs.

Emissive transition metal complexes bound to DNA have been explored extensively as reporters of structure,[19−27] sequence,[28] nucleotide reactivity,[29] hybridization,[30] cross-linking,[31] drug binding,[32] electron transfer,[33−39] and nucleic acid solvation environment and dynamics in duplexes.[40−43] $[Ru(L)_2(dppz)]^{2+}$ (L = bpy (2,2′-bipyridine), phen (1,10-phenanthroline); dppz = dipyrido[3,2-*a*:2′,3′-*c*]phenazine) complexes exhibit the "light switch" effect, whose luminescence is "turned on" in the presence of DNA.[24−28] The DNA photocleavage by $[Ru(bpy)_3]^{2+}$ and related Ru(II) complexes, including intercalated $[Ru(bpy)_2(dppz)]^{2+}$, is only observed in the presence of O_2, and it likely proceeds via the formation of $^1O_2$ through energy transfer from the excited state of the complex.[44] Since the first reports of the "light switch" effect, numerous mononuclear and bimetallic dppz complexes containing a wide variety of metal centers were reported and typically exhibit strong binding to DNA owing to the intercalation of the dppz ligand (K_b values range from $\sim10^4$ to $\sim10^8$ M^{-1}).[20,45−53] It was shown that bimetallic complexes of dppz also bind strongly to DNA, but the two metal centers in the systems reported to date are not in close proximity and their photoreactivity toward nucleic acids was not explored.[54,55]

Bimetallic complexes that exhibit strong metal−metal interactions often afford reactive excited states that are not

(7) (a) Cohen, S. M.; Lippard, S. J. *Prog. Nucleic Acid Res. Mol. Biol.* **2001**, *67*, 93. (b) Zhang, C. X.; Lippard, S. J. *Curr. Opin. Chem. Biol.* **2003**, *7*, 481.
(8) (a) Fuertes, M. A.; Alonso, C.; Perez, J. M. *Chem. Rev.* **2003**, *103*, 645. (b) Fuertes, M. A.; Castilla, J.; Alonso, C.; Perez, J. M. *Curr. Med. Chem.: Anti-Cancer Agents* **2002**, *2*, 539.
(9) (a) Siddik, Z. H. *Cancer Treat. Res.* **2002**, *112*, 263−284. (b) Siddik, Z. H. *Oncogene* **2003**, *22*, 7265.
(10) DeRosa, M. C.; Crutchley, R. J. *Coord. Chem. Rev.* **2002**, *233*−*234*, 351.
(11) Dalla V., Lisa; M., Sebastiano M. *Curr. Med. Chem.* **2001**, *8*, 1405.
(12) Allen, C. M.; Sharman, W. M.; van Lier, J. E. *Tumor Targeting Cancer Ther.* **2002**, 329.
(13) Hsi, R. A.; Rosenthal, D. I.; Glatstein, E. *Drugs* **1999**, *57*, 725.
(14) McCaughan, J. S., Jr. *Drugs Aging* **1999**, *15*, 49.
(15) Jones, B. U.; Helmy, M.; Brenner, M.; Serna, D. L.; Williams, J.; Chen, J. C.; Milliken, J. C. *Clin. Lung Cancer* **2001**, *3*, 37.
(16) Guppy, M. *Biochem. Biophys. Res. Commun.* **2002**, *299*, 676.
(17) Harris, A. L. *Nat. Rev. Cancer* **2002**, *2*, 38.
(18) Knowles, H. J.; Harris, A. L. *Breast Cancer Res.* **2001**, *3*, 318.
(19) Holmlin, R. E.; Tong, R. T.; Barton, J. K. *J. Am. Chem. Soc.* **1998**, *120*, 9724.
(20) Holmlin, R. E.; Yao, J. A.; Barton, J. K. *Inorg. Chem.* **1999**, *38*, 174.
(21) Stoeffer, H. D.; Thornton, N. B.; Temkin, S. L.; Schanze, K. S. *J. Am. Chem. Soc.* **1995**, *117*, 7119.
(22) McMillin, D. R.; Liu, F.; Meadows, K. A. *Coord. Chem. Rev.* **1994**, *132*, 105.
(23) Murphy, C. J.; Mahtab, R.; Caswell, K.; Gearheart, L. A.; Jana, N.; Hammami, S.; Best, D. D. *Proc. SPIE* **2001**, *4258*, 25.
(24) Olson, E. J. C.; Hu, D.; Hörmann, A.; Jonkman, A. M. *J. Am. Chem. Soc.* **1997**, *119*, 11458.
(25) Turro, C.; Bossmann, S. H.; Jenkins, Y.; Barton, J. K.; Turro, N. J. *J. Am. Chem. Soc.* **1995**, *117*, 9026.
(26) (a) Friedman, A. E.; Chambron, J. C.; Sauvage, J. P.; Turro, N. J.; Barton, J. K. *J. Am. Chem. Soc.* **1990**, *112*, 4960. (b) Jenkins, Y.; Friedman, A. E.; Turro, N. J.; Barton, J. K. *Biochemistry* **1992**, *31*, 10809.
(27) (a) Tuite, E.; Lincoln, P.; Nordén, B. *J. Am. Chem. Soc.* **1997**, *119*, 239−240. (b) Lincoln, P.; Broo, S.; Nordén, B. *J. Am. Chem. Soc.* **1996**, *118*, 2644−2653. (c) Haq, I.; Lincoln, P.; Suh, D.; Norden, B.; Chowdhry, B. Z.; Chaires, J. B. *J. Am. Chem. Soc.* **1995**, *117*, 4788.
(28) Holmlin, R. E.; Stemp, E. D. A.; Barton, J. K. *Inorg. Chem.* **1998**, *37*, 29.
(29) Kim, J.; Sistare, M. F.; Carter, P. J.; Thorp, H. H. *Coord. Chem. Rev.* **1998**, *171*, 341.
(30) Joshi, H. S.; Tor, Y. *Chem. Commun.* **2001**, 549.
(31) Copeland, K. D.; Lueras, A. M. K.; Stemp, E. D. A.; Barton, J. K. *Biochemistry* **2002**, *41*, 12785.
(32) Peyratout, C. S.; Aldridge, T. K.; Crites, D. K.; McMillin, D. R. *Inorg. Chem.* **1995**, *34*, 4484.
(33) (a) Delaney, S.; Pascaly, M.; Bhattacharya, P. K.; Han, K.; Barton, J. K. *Inorg. Chem.* **2002**, *41*, 1966. (b) O'Neill, M. A.; Becker, H.-C.; Wan, C.; Barton, J. K.; Zewail, A. H. *Angew. Chem., Int. Ed.* **2003**, *42*, 5896.
(34) Turro, N. J.; Barton, J. K. *J. Biol. Inorg. Chem.* **1998**, 201.
(35) (a) Lewis, F. D.; Wu, T.; Zhang, Y.; Letsinger, R. L.; Greenfield, S. R.; Wasielewski, M. R. *Science* **1997**, *227*, 673. (b) Lewis, F. D.; Liu, J.; Zuo, X.; Hayes, R. T.; Wasielewski, M. R. *J. Am. Chem. Soc.* **2003**, *125*, 4850.
(36) Bhattacharya, P. K.; Barton, J. K. *J. Am. Chem. Soc.* **2001**, *123*, 8649.
(37) Wagenknecht, H.-A.; Rajski, S. R.; Pascaly, M.; Stemp, E. D. A.; Barton, J. K. *J. Am. Chem. Soc.* **2001**, *123*, 4400.
(38) Holmlin, E. R.; Dandliker, P. J.; Barton, J. K. *Angew. Chem., Int. Ed.* **1998**, *36*, 2715.
(39) (a) Krider, E. S.; Meade, T. J. *J. Biol. Inorg. Chem.* **1998**, 222−225. (b) Frank, N. L.; Meade, T. J. *Inorg. Chem.* **2003**, *42*, 1039.
(40) Kang, J. S.; Lakowicz, J. R.; Piszczek, G. *Arch. Pharm. Res.* **2002**, *25*, 143.
(41) (a) Brauns, E. B.; Murphy, C. J.; Berg, M. A. *J. Am. Chem. Soc.* **1998**, *120*, 2449. (b) Brauns, E. B.; Madaras, M. L.; Coleman, R. S.; Murphy, C. J.; Berg, M. A. *Phys. Rev. Lett.* **2002**, *88*, 158101. (c) Gearheart, L. A.; Somoza, M. M.; Rivers, W. E.; Murphy, C. J.; Coleman, R. S.; Berg, M. A. *J. Am. Chem. Soc.* **2003**, *125*, 11812.
(42) Murtaza, Z.; Malak, H. M.; Lakowicz, J. R. In *Advances in Fluorescence Sensing Technology IV*; Proceedings of SPIE Vol. 3602; SPIE: Bellingham, WA, 1999; p 316.
(43) Nair, R. B.; Cullum, B. M.; Murphy, C. J. *Inorg. Chem.* **1997**, *36*, 962.
(44) (a) Fu, P. K.-L.; Bradley, P. M.; van Loyen, D.; Dürr, H.; Bossmann, S. H.; Turro, C. *Inorg. Chem.* **2002**, *41*, 3808. (b) Bradley, P. M.; Turro, C. Unpublished results.
(45) Yam, V. W.-W.; Lo, K. K.-W.; Cheung, K.-K.; Kong, R. Y.-C. *J. Chem. Soc., Dalton Trans.* **1997**, 2067.
(46) Collins, J. G.; Aldrich-Wright, J. R.; Greguric, I. D.; Pellegrini, P. A. *Inorg. Chem.* **1999**, *38*, 5502.
(47) Arounaguiri, S.; Maiya, B. G. *Inorg. Chem.* **1996**, *35*, 4267.
(48) (a) Thomas, A. M.; Neelakanta, G.; Mahadevan, S.; Nethaji, M.; Chakravarty, A. R. *Eur. J. Inorg. Chem.* **2002**, 2720. (b) Dhar, S.; Reddy, P. A. N.; Nethaji, M.; Mahadevan, S.; Saha, M. K.; Chakarvarty, A. R. *Inorg. Chem.* **2002**, *41*, 3469.
(49) Jin, L.; Yang, P. *Polyhedron* **1997**, *16*, 3395.
(50) Che, C.-M.; Yang, M.; Wong, K.-H.; Chan, H.-L.; Lam, W. *Chem.*−*Eur. J.* **1999**, *5*, 3350.
(51) Nair, R. B.; Teng, E. S.; Kirkland, S. L.; Murphy, C. J. *Inorg. Chem.* **1998**, *37*, 139.
(52) Jin, L.; Yang, P. *Microchem. J.* **1998**, *58*, 144.
(53) Metcalfe, C.; Webb, M.; Thomas, J. A. *Chem. Commun.* **2002**, 2026.
(54) (a) McFadyen, W. D.; Wakelin, L. P. G.; Roos, I. A. G.; Hillcoat, B. L. *Biochem. J.* **1986**, *238*, 757. (b) McFadyen, W. D.; Wakelin, L. P. G.; Roos, I. A. G.; Hillcoat, B. L. *Biochem. J.* **1987**, *242*, 177.
(55) (a) Onfelt, B.; Lincoln, P.; Norden, B. *J. Am. Chem. Soc.* **1999**, *121*, 10846. (b) Onfelt, B.; Lincoln, P.; Norden, B. *J. Am. Chem. Soc.* **2001**, *123*, 3630.

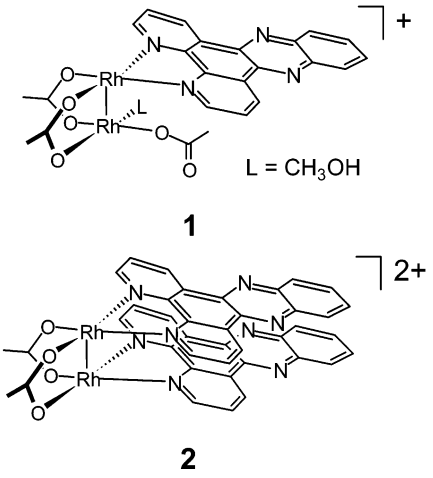

Figure 1. Schematic representations of the molecular structures of **1** and **2**.

available in mononuclear complexes. For example, hydrogen abstraction from the DNA backbone upon photoexcitation of $[Pt_2(pop)_4]^{4-}$ ($pop^{2-} = HO_2POPO_2H^{2-}$) was reported, which results in DNA cleavage.[56,57] The cleavage of duplex DNA by the triplet excited state of $[Pt_2(pop)_4]^{4-}$ is not enhanced by piperidine treatment, consistent with hydrogen abstraction rather than with a mechanism involving guanine oxidation.[58] In model systems, it was shown that $[Pt_2(pop)_4]^{4-}$ reacts with nucleic acids and nucleotides through 4′- and 5′-hydrogen abstraction from the deoxyribose backbone.[56] The overall negative charge of the complex, however, precludes it from binding to the double helix, thereby slowing the bimolecular rate of photocleavage which renders the process inefficient. To circumvent electrostatic repulsion between anionic complexes and DNA, neutral and cationic dirhodium complexes were explored as agents for DNA photocleavage. Complexes of the type $Rh_2(O_2CCH_3)_4(L)_2$ (L = alcohols, PPh_3, py, THF, H_2O) possess long-lived excited states ($\tau = 3.5-5.0$ μs) that can be accessed with visible light (500−700 nm).[59] $Rh_2(O_2CCH_3)_4(OH_2)_2$ exhibits weak DNA binding ($K_b = 4.6 \times 10^2$ M^{-1})[60] and has been shown to photocleave DNA only in the presence of electron acceptors.[61]

To increase the DNA binding of dirhodium complexes and attain direct DNA photocleavage, the photoreactive dirhodium(II) core was combined with intercalating dppz ligands. This work describes the synthesis and characterization of *cis*-$[Rh_2(\mu\text{-}O_2CCH_3)_2(dppz)(\eta^1\text{-}O_2CCH_3)(CH_3OH)]^+$ (**1**) and *cis*-$[Rh_2(\mu\text{-}O_2CCH_3)_2(dppz)_2]^{2+}$ (**2**), whose structures are schematically depicted in Figure 1. The DNA binding and photocleavage properties of the complexes were measured in vitro, and the results were correlated to the differences in the cytotoxicity and photocytotoxcity of **1** and **2** toward human skin cells.

Experimental Section

Materials. Sodium chloride, sodium phosphate, gel loading buffer (0.05% (w/v) bromophenol blue, 40% (w/v) sucrose, 0.1 M EDTA (pH = 8.0), 0.5% (w/v) sodium lauryl sulfate), Tris base, Tris/HCl, and ethidium bromide were purchased from Sigma and used as received. Calf thymus DNA was purchased from Sigma and was dialyzed against a 5 mM Tris, 50 mM NaCl (pH = 7.5) buffer three times during a 48 h period prior to use. The pUC18 plasmid was purchased from Bayou Biolabs and purified using the Concert Miniprep System from Life Technology. *Sma*I was purchased from Invitrogen and used as received. Acetonitrile and dichloromethane were dried over 3 and 4 Å molecular sieves, respectively, and distilled under a nitrogen atmosphere prior to use. All reactions were carried out under nitrogen using standard Schlenk techniques. The reagents $RhCl_3$, sodium acetate, $NaBF_4$, and polystyrene sulfonate (PSS) were purchased from Aldrich and used without further purification. The compounds $Rh_2(\mu\text{-}O_2CCH_3)_4(CH_3CN)_2$ and dppz (dppz = dipyrido[3,2-*a*:2′,3′-*c*]phenazine) were synthesized by previously reported methods.[62−65]

***cis*-[Rh$_2$(μ-O$_2$CCH$_3$)$_2$(dppz)(η^1-O$_2$CCH$_3$)(CH$_3$OH)](O$_2$CCH$_3$) (1).** A suspension of dppz (53.8 mg, 0.19 mmol) in CH_2Cl_2 was added to a slurry of $Rh_2(\mu\text{-}O_2CCH_3)_4(CH_3CN)_2$ (100 mg, 0.19 mmol) in CH_2Cl_2. The mixture was stirred for 36 h under refluxing conditions, and the resulting green precipitate was filtered and washed with CH_2Cl_2. The product was suspended in methanol and stirred for 24 h at room temperature. The solution was concentrated, and diethyl ether was added to precipitate a green solid, which was collected by filtration (91% yield). FAB mass spectrum: $m/z = 664.88$ ($[Rh_2(\mu\text{-}O_2CCH_3)_2(dppz)(O_2CCH_3)]^+$). ^{1}H NMR (300 MHz) in $CDCl_3/CD_3OD$ (1:1 v:v), δ/ppm (mult, int, assignment): 1.11 (s, 3H, CH_3CO_2), 1.88 (s, 3H, CH_3CO_2), 2.35 (s, 3H, CH_3CO_2), 2.41 (s, 3H, CH_3CO_2), 8.15 (m, 4H, dppz), 8.51 (m, 2H, dppz), 8.88 (dd, 2H, dppz), 9.79 (dd, 2H, dppz). UV−vis in H_2O, λ/nm (ϵ/M^{-1} cm^{-1}): 278 (57 870), 360 (11 730), 428 (3177), 590 (354).

***cis*-[Rh$_2$(μ-O$_2$CCH$_3$)$_2$(dppz)$_2$]$^{2+}$ (2).** A solution of $Rh_2(\mu\text{-}O_2CCH_3)_4(CH_3CN)_2$ (100 mg, 0.19 mmol) in acetonitrile was treated with solid dppz (107.7 mg, 0.38 mmol), and the suspension was heated to reflux for 24 h. After this time period, the red mixture was cooled to room temperature, filtered, and washed with acetonitrile to afford a red solid (93% yield). Subsequent crystallization from a methanol/benzene/diethyl ether solution in an excess of $NaBF_4$ produced crystals suitable for X-ray characterization. FAB mass spectrum: $m/z = 443.98$ ($[Rh_2(\mu\text{-}O_2CCH_3)_2(dppz)_2]^{2+}$). ^{1}H NMR of the diacetate salt (300 MHz) in $CDCl_3/CD_3OD$ (1:1 v:v), δ/ppm (mult, int, assignment): 1.75 (s, 6H, CH_3CO_2), 2.67 (s, 6H, CH_3CO_2), 7.73 (m, 4H, dppz), 7.81 (m, 4H, dppz), 7.90 (m, 4H, dppz), 8.64 (d, 4H, dppz), 9.05 (d, 4H, dppz). UV−vis in H_2O, λ/nm (ϵ/M^{-1} cm^{-1}): 203 (69 390), 276 (86 430), 363 (15 170), 434 (5459).

Methods. For the X-ray crystallographic analysis, a red prismatic crystal of **2** (approximate dimensions: $0.17 \times 0.08 \times 0.22$ mm^3) was selected. The crystal was coated with Paratone oil, transferred to a nylon loop, and placed in a cold N_2 stream at 110(2) K. An

(56) (a) Breiner, K. M.; Daugherty, M. A.; Oas, T. G.; Thorp, H. H. *J. Am. Chem. Soc.* **1995**, *117*, 11673. (b) Kalsbeck, W. A.; Gingell, D. M.; Malinsky, J. E.; Thorp, H. H. *Inorg. Chem.* **1994**, *33*, 3313.
(57) Klasbeck, W. A.; Grover, N.; Thorp, H. H. *Angew. Chem., Int. Ed. Engl.* **1991**, *30*, 1517.
(58) Carter, P. J.; Breiner, K. M.; Thorp, H. H. *Biochemistry* **1998**, *37*, 13736.
(59) Bradley, P. M.; Bursten, B. E.; Turro, C. *Inorg. Chem.* **2001**, *40*, 1376.
(60) Sorasaenee, K.; Fu, P. K.-L.; Angeles-Boza, A. M.; Dunbar, K. R.; Turro, C. *Inorg. Chem.* **2003**, *42*, 1267.
(61) Fu, P. K.-L.; Bradley, P. M.; Turro, C. *Inorg. Chem.* **2001**, *40*, 2476.
(62) Rempel, G. A.; Legzdins, P.; Smith, H.; Wilkinson, G. *Inorg. Synth.* **1972**, *13*, 90.
(63) Winkhaus, G.; Ziegler, P. *Z. Anorg. Allg. Chem.* **1967**, *350*, 51.
(64) Yamada, M.; Tanaka, Y.; Yoshimoto, Y. *Bull. Chem. Soc. Jpn.* **1992**, *65*, 1006.
(65) Dickeson, J. E.; Summers, L. A. *Aust. J. Chem.* **1970**, *23*, 1023.

indexing of the preliminary diffraction patterns indicated that the crystal was monoclinic. A total of 17 935 reflections were collected in the range $2.40 \leq \theta \leq 27.49°$. The data collection covered approximately a hemisphere of reciprocal space, by a combination of three or four sets of exposures; each set had a different ϕ angle for the crystal, and each exposure covered 0.3° in Ω. Crystal decay, which was monitored by analyzing duplicate reflections, was found to be less than 1%; therefore, no decay correction was applied. During the final cycles of refinement, all atoms with the exception of hydrogen were refined anisotropically. Hydrogen atoms belonging to hydroxo groups were placed in suitable positions with idealized tetrahedral X−O−H geometries. Hydrogen atoms belonging to methyl groups were placed in regions of maximum electron density around the methyl C atoms, and the torsional angles were refined with idealized C−H distances and tetrahedral angles. The structure was solved and refined in the chiral space group $P2_1$. The asymmetric unit contains the cationic *cis*-$[Rh_2(\mu\text{-}O_2CCH_3)_2(dppz)_2]^{2+}$ molecule with an ethanol molecule and an acetate ion coordinated to the axial positions, one ethanol solvent molecule of crystallization, and a $[BF_4]^-$ anion that refined to full occupancy. The bond distances and angles were idealized during refinement with the hydrogen *U* values set at 1.2 or 1.5 times the equivalent isotropic *U* of the atoms to which they are attached. The final refinement cycle was based on 6822 unique reflections (6192 with $F_o^2 > 2\sigma(F_o^2)$), 627 parameters, and 85 restraints (R1 = 0.0389, wR2 = 0.0688). The maximum and minimum peaks in the final difference Fourier map corresponded to 0.74 and −0.71 e/Å^3, respectively, with a goodness-of-fit value of 1.022.

Solutions containing only 100 μM calf-thymus DNA and with 20 μM of either **1** or **2** (1 mM phosphate buffer, 2 mM NaCl, pH = 7.2) were used to determine the melting temperatures. The DNA photocleavage experiments were carried out using 20 μL of total sample volume in 0.5 mL transparent Eppendorf tubes containing 100 μM pUC18 plasmid and various concentrations of each metal complex. Irradiation of the solutions was performed either in air, under positive pressure of argon or nitrogen following bubbling for ∼15 min, or after 5 freeze−pump−thaw cycles in quartz tubes equipped with a Kontes stopcock (using ∼3-fold greater solution volume). Following irradiation, 4 μL of the DNA gel loading buffer was added to each 20 μL sample. The electrophoresis was carried out using either 1% or 2% agarose gel stained with 0.5 mg/L eithidium bromide in 1× TAE buffer (40 mM tris-acetate, 1 mM EDTA, pH ∼ 8.2); other conditions are specified as needed.

The binding constants of the metal complexes to calf thymus DNA determined by optical titrations at room temperature were measured with 5 μM metal complex, and the calf thymus DNA concentration was varied from 0 to 100 μM (5 mM Tris/HCl, pH 7.5). The dilution of metal complex concentration at the end of each titration was negligible. The DNA binding constant, K_b, was obtained from fits of the titration data to eq 1,[51,66]

$$\frac{\epsilon_a - \epsilon_f}{\epsilon_b - \epsilon_f} = \frac{b - (b^2 - 2K_b{}^2C_t[\mathrm{DNA}]_t/s)^{1/2}}{2K_bC_t} \qquad (1)$$

where $b = 1 + K_bC_t + K_b[\mathrm{DNA}]_t/2s$, C_t and $[\mathrm{DNA}]_t$ represent the total complex and DNA concentrations, respectively, *s* is base pair binding site size, and ϵ_a, ϵ_f, and ϵ_b represent the apparent, free complex, and bound complex molar extinction coefficients, respectively. The value of ϵ_b was determined from the plateau of the DNA titration, where addition of DNA did not result in further changes to the absorption spectrum.

In the binding constant determination using dialysis, the total concentration of metal complex, C_t, present in the dialysate solution was determined spectrophotometrically using its extinction coefficient. The DNA (100 μM) was placed in a dialysis membrane and was dialyzed against 1.0 L of 10 μM metal complex in circulating buffer (6 mM Na_2HPO_4, 3 mM NaH_2PO_4, 1 mM EDTA, and 125 mM NaCl, pH = 7.0) for 48 h. The free complex concentration (C_f) was determined from an aliquot of the dialysate solution following the 48 h equilibration period. The amount of complex bound to the DNA, C_b, was determined from the mass balance equation given by $C_b = C_t - C_f$.

Human skin fibroblasts (Hs-27) were obtained from the American Type Culture Collection, cell line CRL-1634 (Manassas). Cells were cultured in Dulbecco's modified Eagle medium, containing 10% fetal bovine serum (Life Technologies), 50 μg/mL gentamicin, 4.5 mg/mL glucose, and 4 mM L-glutamine (Invitrogen Life Technology). Cell cultures were incubated in a humidified atmosphere containing 5% CO_2 at 37 °C. For assessing the cytotoxicity and photocytotoxicity of different compounds, subconfluent (50−80% confluent) monolayers of Hs-27 in 60 mm culture dishes were used. The monolayers were washed twice with phosphate-buffered saline (PBS) to ensure that the culture dishes were free of any culture medium, and then fresh PBS containing different concentrations of each compound was added to cover the fibroblasts. The cells were irradiated through the PBS buffer, which does not absorb light in the visible region.

After irradiation, the cells were removed from the dishes by trypsinization, seeded into 24-well culture dishes, and incubated for 2−4 days or until the untreated control group reached confluence. *N*-Lauroyl sarcosine (200 μL, 40 mM) was then added to each well, and the cells were allowed to lyse for at least 15 min. Quantitative determination of the protein content in each well was undertaken using Peterson's modification of the micro-Lowry method (Sigma reagent kit),[67] where the lysate was treated with 200 μL of Lowry reagent for 20 min and then with 100 μL of Folin−Ciocalteau phenol reagent for 30 min or until color developed. A portion of the contents (200 μL) of each well was transferred to a 96-well plate for absorbance determination using a multiwell plate reader (Dynatech Laboratory). The absorbance at 630 nm was monitored, which is proportional to the total protein content and the number of cells in each well.[67]

Instrumentation. The ^{1}H NMR spectra of **1** and **2** were recorded on a Unity-300 NMR spectrometer. Absorption measurements were performed either on a Schimadzu UVPC-3001 spectrophotometer or on a Hewlett-Packard diode array spectrometer (HP 8453) with HP8453 Win System software equipped with a Peltier temperature-controlled sample cell and driver (HP89090A) for thermal denaturation studies. The relative changes in viscosity were measured on a Cannon-Manning semi-micro viscometer for transparent liquids. The viscometer was immersed in a constant temperature water bath (24 °C) controlled by a Neslab (model RGE-100) circulator. The ethidium bromide stained agarose gels were imaged using a GelDoc 2000 transilluminator (BioRad) equipped with Quality One (v. 4.0.3) software.

X-ray diffraction data were collected on a Bruker APEX CCD diffractometer with graphite-monochromated Mo Kα radiation (λ = 0.710 73 Å). The frames were integrated with the Bruker SAINT software,[68] and a semiempirical absorption correction using multiple-

(66) Pyle, A. M.; Rehman, J. P.; Mehoyrer, R.; Kumar, C. V.; Turro, N. J.; Barton, J. K. *J. Am. Chem. Soc.* **1989**, *111*, 3051.

(67) (a) Peterson, G. L. *Anal. Biochem.* **1977**, *83*, 346. (b) Bensadoun, A.; Weinstein, D. *Anal. Biochem.* **1976**, *70*, 241. (c) Lowry, O. H.; Roseberough, N. J.; Farr, A. L.; Randall, R. J. *J. Biol. Chem.* **1951**, *193*, 265.

(68) *SAINT*, version 6.34; Bruker AXS Inc.: Madison, WI, 2001.

measured reflections was applied using SADABS.[69] The structures were solved and refined using X-SEED,[70] a graphical interface to SHELX97.[71]

The DNA photocleavage experiments were conducted using a 150 W Xe arc lamp in a PTI housing (Milliarc Compact Lamp Housing) as the light source powered by an LPS-220 power supply (PTI) with an LPS-221 igniter (PTI). The wavelength of the light reaching the samples was controlled by placing high-pass colored glass filters (Melles Griot) and a 10 cm water cell in the light path. Irradiation of cell cultures was accomplished through the use of two 40 W GE watt-miser bulbs (General Electric) with an Acrylite OP-3 high-pass filter, keeping the total irradiation below 5 J/cm^2 and providing a broad-band source of irradiation (400−700 nm). It should be noted that cell irradiation intensities greater than 5 J/cm^2 have been shown to result in concomitant cell death in the absence of any external agents and should therefore be avoided when testing compounds with potential applications to live tissue.[72]

Results and Discussion

Synthesis and Characterization. The complex $Rh_2(\mu\text{-}O_2CCH_3)_4(CH_3CN)_2$ reacts with 1 and 2 equiv of dppz (dppz = dipyrido[3,2-*a*:2′,3′-*c*]phenazine) to yield *cis*-$[Rh_2(\mu\text{-}O_2CCH_3)_2(dppz)(\eta^1\text{-}O_2CCH_3)(CH_3OH)]^+$ (**1**) and *cis*-$[Rh_2(\mu\text{-}O_2CCH_3)_2(dppz)_2]^{2+}$ (**2**), respectively (Figure 1). Characterization of **1** was achieved by ^{1}H NMR spectroscopy in $CDCl_3/CD_3OD$ and FAB mass spectrometry. Four different acetate resonances were observed in the structure of C_1 symmetry, corresponding to two in bridging positions, one coordinated to one rhodium atom in a terminal fashion, and the third as an unbound counterion. The aromatic dppz resonances of **1** appear at 8.15, 8.51, 8.88, 8.64, and 9.79 ppm and are typical for a coordinated dppz ligand.[73,74]

The molecular structure of **2**, determined by X-ray crystallographic methods, consists of a dinuclear Rh_2(II,II) core with a pair of chelating dppz ligands coordinated to each Rh atom in a syn disposition and two bridging acetates occupying the remaining equatorial sites. An acetate ion and a CH_3OH group coordinated at the axial positions completes an irregular octahedral coordination sphere about each Rh atom. The structure of the dinuclear cation in **2** is shown in Figure 2 and is similar to those reported for related dirhodium complexes.[75,76] The Rh−Rh distance in **2**, 2.5519(6) Å, is similar to those reported for $[Rh_2(O_2CCH_3)_4(L)_2]^{2+}$ (L = bpy, phen, 4,7-dimethyl-phen, 3,4,7,8-tetramethyl-phen), 2.548(4), 2.5557(4), 2.565(1), and 2.564(1) Å, respectively.[75,76] Similarly, in *cis*-$[Rh_2(O_2CCF_3)_2(bpy)_2]^{2+}$ a Rh−Rh distance of 2.570(6) Å was reported.[75] The Rh−N bond lengths in **2**, which range from 2.005(4) to 2.016(4) Å, are also comparable to those observed in the analogous bpy, phen, and substituted phen complexes.[75]

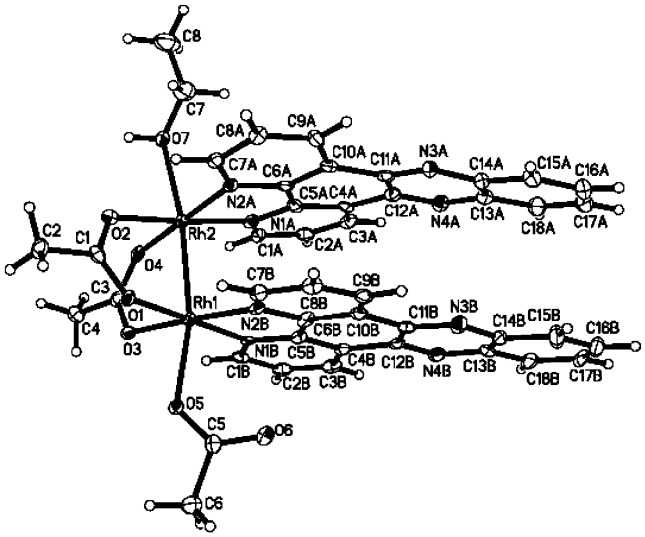

Figure 2. Thermal ellipsoid plot of molecular dication **2**.

A striking feature of **2** is the close proximity of the two dppz ligands, with a nearly eclipsed conformation across the metal−metal bond dictated by the rigid bridging acetate groups. In the absence of bridging ligands, a staggered conformation about a Rh−Rh single bond is expected, since no electronic barrier to rotation is present. The internal twist angle away from the eclipsed geometry of 13° in **2** is significantly greater than that observed for the bis-bpy analogue (6.2°) but similar to those in the corresponding phen and substituted phen complexes (16−20°).[75,76] The dihedral torsional angle defined by the two planes normal to the three aromatic rings of both dppz ligands closest to the metal is 15.1(2)°. Similar values were observed in $[Rh_2(O_2CCH_3)_2(bpy)_2]^{2+}$ (15.8°) and $[Rh_2(O_2CCH_3)_2(L)_2]^{2+}$ (L = bpy, phen, 4,7-dimethyl-phen, 3,4,7,8-tetramethyl-phen), with deviations that range from 9.0 to 10.4°.[76]

The splaying of the dppz ligands from a parallel orientation and the twisting from an eclipsed geometry serve to reduce steric interactions between the ligands, since the short Rh−Rh bond distance would otherwise bring them closer than is favorable for $\pi-\pi$ stacking interactions.[77] Since the dppz ligands are distorted, and their best least-squares planes are not exactly parallel to each other, a unique interplanar distance cannot be defined for these ligands. The shortest nonbonded atomic contacts, however, provide an indication of the separation of the two dppz ligands in this molecule, with 3.494(7) Å being the shortest distance between the outermost rings. The shortest atomic contacts between dppz ligands occur closest to the metal−metal bond, with atomic distances for N1A···N1B, C7A···C7B, N2A···N2B, and C1A···C1B of 3.050(5), 3.289(5), 3.058(5), and 3.242(5) Å, respectively.

The ^{1}H NMR spectrum in $CDCl_3/CD_3OD$ (1:1, v:v) is consistent with retention of the solid-state structure of **2**

(69) *SADABS*, version 2.03; Bruker AXS Inc.: Madison, WI, 2002.
(70) Barbour, L. J. *J. Supramol. Chem.* **2001**, *1*, 189.
(71) Sheldrick, G. M. *SHELX, Programs for Solving and Refining Crystal Structures*; University of Göttingen: Göttingen, Germany, 1997.
(72) Kornhauser, A., Wamer, W. G.; Lambert, L. A. In *Dermatotoxicology*; Marzulli, F. N., Maibach, H. I., Eds.; Taylor & Francis: Washington, DC, 2002; pp 189−230.
(73) Chambron, J.-C.; Sauvage, J.-P.; Amouyal, E.; Koffi, P. *New J. Chem.* **1985**, *9*, 527.
(74) Liu, J.-G.; Zhang, Q.-L.; Shi, X.-F.; Ji, L.-N. *Inorg. Chem.* **2001**, *40*, 5045.
(75) Crawford, C. A.; Matonic, J. H.; Streib, W. E.; Huffman, J. C.; Dunbar, K. R.; Christou, G. *Inorg. Chem.* **1993**, *32*, 3125.
(76) Calligaris, M.; Campana, L.; Mestroni, G.; Tornatore, M.; Alessio, E. *Inorg. Chim. Acta* **1987**, *127*, 103.
(77) Hunter, C. A.; Sanders, J. K. M. *J. Am. Chem. Soc.* **1990**, *112*, 5525.

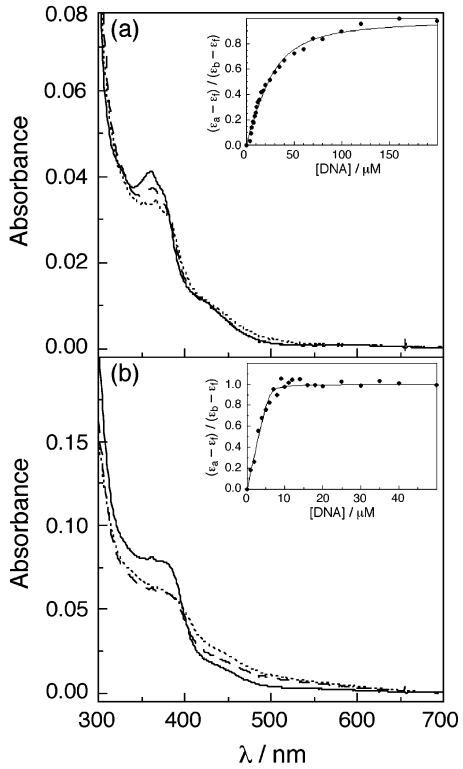

Figure 3. Electronic absorption spectra of 5 μM (a) **1** and (b) **2** in 5 mM Tris (pH = 7.5) in water (—) and in the presence of 100 μM calf-thymus DNA (---) and 100 μM PSS (— —). Insets: fits of the absorption to eq 1 for (a) 6.2 μM **1** and (b) 3.2 μM **2** (see text).

dissolved in this mixture. Two acetate resonances are observed at 1.75 and 2.67 ppm corresponding to two free and two bridging acetates, respectively.[78] The aromatic dppz protons appear at 7.73, 7.81, 7.90, 8.64, and 9.05 ppm and are shifted upfield compared to those of **1**. This shift can be attributed to additional shielding of the dppz protons due to the close proximity of the second dppz ligand. Similar shifts of the aromatic protons were observed for *cis*-$[Rh_2(\mu\text{-}O_2CCH_3)_2(L)_2]^{2+}$ (L = bpy, phen), whose structures parallel that of **2**.[75] The ^{1}H NMR spectrum of **2** in solution is consistent with an eclipsed C_{2v} symmetry of the ligands, indicating a dynamic process involving rotational oscillation about the Rh−Rh bond.

Electronic Absorption and DNA Binding. The electronic absorption spectra of **1** and **2** in 5 mM Tris, 50 mM NaCl (pH = 7.0) are shown in Figure 3 and are similar to those recorded in water. The absorption at 360 nm (ϵ = 11 700 M^{-1} cm^{-1}) and 363 nm (ϵ = 15 200 M^{-1} cm^{-1}) observed in **1** and **2**, respectively, can be assigned as arising from a dppz $\pi\pi^*$ ligand-centered (LC) transition. This LC transition at ~360 nm has also been observed in various dppz transition metal complexes.[20,51] In both complexes the absorption tails off into the visible region, with a maximum at 428 nm (ϵ = 3180 M^{-1} cm^{-1}) in **1** and at 434 nm (ϵ = 5460 M^{-1} cm^{-1}) in **2**. Similar transitions are also observed in the corresponding complexes of bpy at 424 nm (ϵ = 2010 M^{-1} cm^{-1}) in $[Rh_2(\mu\text{-}O_2CCH_3)_2(\eta^1\text{-}O_2CCH_3)(CH_3OH)(bpy)]^+$ and 432 nm (ϵ = 2080 M^{-1} cm^{-1}) in $[Rh_2(\mu\text{-}O_2CCH_3)_2(bpy)_2]^{2+}$,[75,76] as well as in $[Rh_2(\mu\text{-}O_2CCH_3)_2(L)_2]^{2+}$ (L = substituted 2,2′-bipyrine, 1,10-phenanthroline).[75] A weaker transition was observed for $Rh_2(O_2CCH_3)_4$ at 443 nm (ϵ = 112 M^{-1} cm^{-1}) in water, previously assigned to Rh−Rh(π^*) → Rh−O(σ^*).[75,76] Since the intensities of the absorptions at similar energies in **1** and **2** are ~30- and ~50-fold greater than the corresponding transition for $Rh_2(O_2CCH_3)_4$, it is possible that these transitions in **1** and **2** are charge transfer in nature and involve the dppz ligands. The weak absorption at λ > 500 nm in each complex is believed to arise from metal-centered (MC) transitions associated with the bimetallic core, since they are also observed in $Rh_2(O_2CCH_3)_4$ and *cis*-$[Rh_2(\mu\text{-}O_2CCH_3)_2(L)_2]^{2+}$ (L = bpy, phen).[75,79−81] In $Rh_2(O_2CCH_3)_4$, the transition at 585 nm (ϵ = 235 M^{-1} cm^{-1}) has been assigned to Rh−Rh(π^*) → Rh−Rh(σ^*).[75,76]

In water, negative deviations from Beer's law are observed for **1** and **2** at concentrations greater than 20 μM (360 nm) and 5 μM (363 nm), respectively. These deviations are likely due to intermolecular π-stacking of the dppz ligands, which are commonly observed for organic aromatic compounds and metal complexes with hydrophobic ligands in water.[82,83] The aggregation appears to be more pronounced for the bis-dppz complex, **2**, than for **1**, consistent with the more hydrophobic nature of the former arising from the presence of a second dppz ligand in the coordination sphere.

The spectral changes of 5 μM solutions (5 mM tris, 50 mM NaCl, pH = 7.5) of **1** and **2** upon addition of 100 μM DNA are shown in Figure 3. Both complexes exhibit pronounced hypochromism of the dppz $\pi\pi^*$ transition, along with a modest bathochromic shift. Binding of 5 μM complex to DNA results in 18% hypochromicity in **1** at 360 nm and 22% in **2** at 363 nm. Similar hypochromicity was reported for $[Ru(NH_3)_4(dppz)]^{2+}$ and $[Ru(phen)_2(dppz)]^{2+}$, which are believed to bind to DNA through intercalation of the dppz ligand with binding constants, K_b, of 1.24 × 10^5 M^{-1} (s = 0.02) and 5.1 × 10^6 M^{-1} (s = 0.6), respectively.[51] Fits of eq 1 using the decrease in the dppz $\pi\pi^*$ absorption as a function of increasing DNA concentration for various concentrations of **1** and **2** in 5 mM Tris (pH = 7.0) result in K_b = 4.4(7) × 10^5 M^{-1}, s = 2.1(3), and K_b = 7.0(9) × 10^6 M^{-1}, s = 0.9-(1), respectively. Typical fits are shown in the insets of Figure 3 for 6.2 μM **1** and 3.2 μM **2** in 5 mM Tris (pH = 7.0). Addition of 50 mM NaCl (5 mM Tris, pH = 7.0) leads to a small decrease in the apparent binding constant of **1**, with K_b = 2.4(9) × 10^5 M^{-1}, s = 1.4(3), and a greater decrease in that of **2**, K_b = 1.3(6) × 10^6 M^{-1}, s = 1.0(3).

Hypochromic and bathochromic shifts of LC transitions for aromatic ligands typically arise from π-stacking interactions in polar solvents, which in this case may result from

(78) Crawford, C. A.; Matonic, J. H., Huffman; J. C., Folting, K.; Dunbar, K. R.; Christou, G. *Inorg. Chem.* **1997**, *36*, 2361.
(79) Boyar, E. B.; Robinson, S. D. *Coord. Chem. Rev.* **1983**, *50*, 109.
(80) Felthouse, T. R. *Prog. Inorg. Chem.* **1982**, *29*, 73.
(81) (a) Miskowski, V. M.; Dallinger, R. F.; Christoph, G. G.; Morris, D. E.; Spies, G. H.; Woodruff, W. H. *Inorg. Chem.* **1987**, *26*, 2127. (b) Trexler, J. W., Jr.; Schreiner, A. F.; Cotton, F. A. *Inorg. Chem.* **1988**, *27*, 3266.
(82) Jones, G., II; Vullev, V. I. *J. Phys. Chem. A* **2001**, *105*, 6402.
(83) Bilakhiya, A. K.; Tyagi, B.; Paul, P.; Natarajan, P. *Inorg. Chem.* **2002**, *41*, 3830.

intercalation between the DNA bases or from the formation of aggregates of the hydrophobic molecules in water.[80−84] It has been previously shown that polyanions facilitate the aggregation of cationic hydrophobic molecules on their surface in aqueous media,[84−87] including those which utilize DNA as a template.[88] The structure of **1** (Figure 1), with a single dppz ligand protruding from the dirhodium core, suggests that the complex should be able to intercalate between the DNA bases without large steric constraints. In contrast, from the distance between the outermost rings of the two dppz ligands in the crystal structure of **2** (3.494(7) Å, Figure 2), it would not be expected that the complex could intercalate between the DNA bases, which are ~3.4 Å apart in B-DNA.[89] Despite these logical predictions, the apparent DNA binding constant obtained from the hypochromicity of the dppz-centered transition (eq 1) of **2** is 16 times greater than that of **1**. The greater ionic strength effect on the binding constant of **2** compared to **1** may be due to greater aggregation of the former on the anionic DNA backbone. Such templated aggregation may be explained by electrostatic binding of the cationic complexes to the phosphate backbone of the host DNA polyanion, coupled to cooperative intermolecular hydrophobic interactions between the dppz ligands. The fitted value of *s*, the number of DNA bases associated with the complex, also provides information on surface aggregation. The values of *s* obtained from the fits range from 1.4 to 2.0 for complex **1**, but values of $s \leq 1$ are obtained for **2**. Aggregation of hydrophobic molecules on the DNA surface result in low values of the binding site size, with $s < 1$.[51] Therefore, both the ionic strength dependence and value of *s* are consistent with greater surface aggregation (π-stacking) of **2** relative to **1** aided by the anionic DNA backbone.

Additional experiments aimed at the elucidation of the possible intercalation and surface aggregation of **1** and **2** were performed. These include optical titrations with PSS (PSS = polystyrene sulfonate), a polyanion that does not support intercalation, shifts in the DNA melting temperature, and changes in viscosity of the DNA solutions in the presence of **1** and **2**.

The spectral changes to solutions of **2** that result from titrations with PSS are nearly superimposable with those observed in the presence of similar concentrations of DNA (Figure 3). Figure 3b shows the absorption changes to a 5 μM solution of **2** (5 mM Tris, pH = 7.0) upon addition of 100 μM PSS and 100 μM DNA, where similar hypochromicity is observed in the presence of both polyanions. Although some spectral changes are evident when a comparable experiment is performed with **1** (Figure 3a), 100 μM DNA results in greater hypochromicity (18%) than PSS (11%). The changes in absorption for both complexes in the presence of PSS can be attributed to enhanced aggregation of **1** and **2** induced by the polyanion; the hypochromicity observed in **2** in the presence of DNA is solely due to surface aggregation driven by electrostatic and hydrophobic interactions, whereas **1** exhibits both surface aggregation and intercalation. This type of aggregation has been shown to take place in aqueous media for cationic hydrophobic molecules and metal complexes with a variety of polyanions, including dendrimers, PSS, and DNA.[80−84]

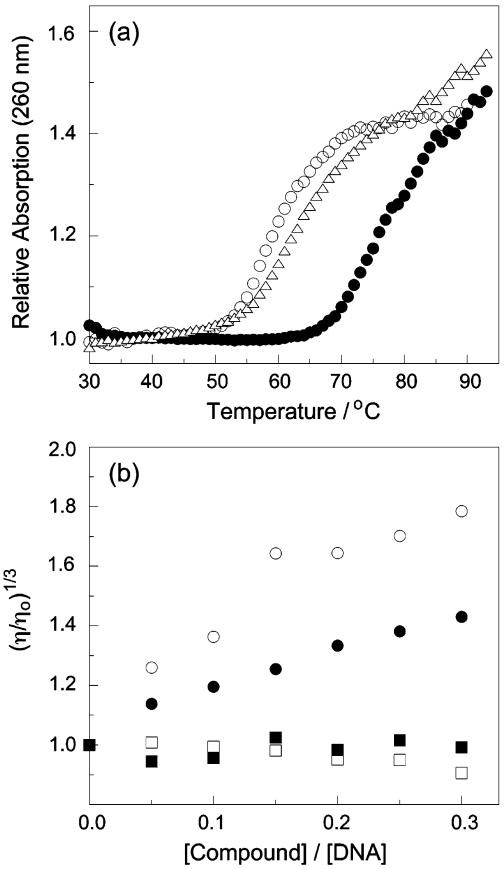

Figure 4. (a) Thermal denaturation of 100 μM calf-thymus DNA (1 mM phosphate, 2 mM NaCl, pH = 7.2) alone (○) and with 20 μM **1** (●) and **2** (△). (b) Relative viscosity changes of solutions containing 200 μM sonicated herring sperm DNA as the concentration of EtBr (○), **1** (●), Hoechst 33258 (□), and **2** (■) is increased.

As shown in Figure 4a, the melting temperature (T_m) of 100 μM calf-thymus DNA in **1** mM phosphate buffer and 2 mM NaCl (pH = 7.2) was measured to be 57 ± 2 °C. A small shift in T_m to 63 ± 2 °C was observed in the presence of 20 μM **2** (Figure 4a). A similar ΔT_m was also observed upon addition of 20 μM $MgCl_2$ (ΔT_m = 5 °C), indicating that the modest shift is due to the presence of a divalent cation and not intercalation. In contrast, Figure 4a shows that the addition of 20 μM **1** to the DNA solution results in a large shift in the melting temperature to 78 ± 2 °C. The large increase in the DNA melting temperature observed for **1**, ΔT_m = 21 °C, is consistent with intercalation of the complex and is similar to that previously measured for the known intercalator $[Rh(phi)_2(phen)]^{3+}$ (phi = 9,10-phenanthrenequinone diimine).[90]

(84) Jockusch, S.; Turro, N. J.; Tomalia, D. A. *Macromolecules* **1995**, *28*, 7416.
(85) Slavnova, T. D.; Chibisov, A. K.; Gorner, H. *J. Phys. Chem. A* **2002**, *106*, 10985.
(86) Karukstis, K. K.; Perelman, L. A.; Wong, W. K. *Langmuir* **2002**, *18*, 10363.
(87) Wang, M. M.; Dilek, I.; Armitage, B. A. *Langmuir* **2003**, *19*, 6449.
(88) Wang, M.; Silva, G. L.; Armitage, B. A. *J. Am. Chem. Soc.* **2000**, *122*, 9977.
(89) Stryer, L. *Biochemistry*, 4th ed.; Freeman and Co.: New York, 1995.

Intercalation of molecules between DNA bases is known to increase the viscosity of the solution owing to unwinding and elongation of the double helix.[91] It is evident from Figure 4b that the addition of **1** to DNA results in an increase in the relative viscosity of the solution, although to a lesser extent than the changes observed for the same concentration of ethidium bromide (EtBr), which is known to intercalate between the DNA bases with $K_b = 1.7 \times 10^5\ M^{-1}$.[92,93] In contrast, similar concentrations of **2**, like the minor groove binder Hoechst 33258, do not result in changes in the relative viscosity (Figure 4b). Since the DNA binding constants measured using dialysis were $1 \times 10^4\ M^{-1}$ and $4 \times 10^3\ M^{-1}$ for **1** and **2** (5−20 μM complex, 90 μM DNA), respectively, the greater increase in viscosity observed for EtBr compared to **1** at each [probe]/[DNA] ratio is likely due to the lower binding constant of the latter to DNA.

The large ΔT_m and increase in viscosity induced by **1** are consistent with its intercalation between the DNA bases, whereas the modest value of ΔT_m and the lack of increase in viscosity support a nonintercalative binding mode for **2**. It should be noted that the DNA binding constants measured using dialysis for **1** and **2** are ∼2−3 orders of magnitude lower than those determined from the optical titrations, which can be explained by the aggregation of **1** and **2** aided by the DNA polyanion. These results clearly show the importance of using several techniques to ascertain intercalation and further underscore the fact that optical titrations alone may result in erroneous assignments of DNA binding modes and binding constants.

DNA Photocleavage. As shown in Figure 5a, both **1** and **2** are able to photocleave plasmid DNA upon absorption of photons in the visible region ($\lambda_{irr} \geq 395$ nm, 15 min). The control lane in Figure 5a (lane 1), which contains 100 μM pUC18 plasmid alone in the dark, shows the position of the undamaged supercoiled pUC18 plasmid (form I) with a small amount of nicked, circular DNA (form II). The migration of cut, linear plasmid (form III) is shown in lane 2 (Figure 5a) for pUC18 plasmid treated with *Sma*I restriction enzyme. It is evident from lanes 3 and 5 (Figure 5a) that exposure of 100 μM pUC18 plasmid to 20 μM **1** and **2** in the dark, respectively, does not result in DNA cleavage. Irradiation of 100 μM pUC18 in the presence of 20 μM **1** and **2** ($\lambda_{irr} \geq$ 395 nm, 15 min) results in the formation of nicked (form II) DNA, as shown in lanes 4 and 6, respectively (Figure 5a). Although complex **2** exhibits ∼30% greater molar absorptivity than **1** at ∼430 nm, greater photocleavage is observed for **1** (lane 4) compared to **2** (lane 6). The difference in the DNA photocleavage may be due to the ability of **1** to intercalate, thus positioning the complex for greater reactivity with the DNA backbone.

Although some of the photocleavage by these complexes observed with $\lambda_{irr} \geq 395$ nm appears to depend on the presence of oxygen, cleavage is still observed in deoxygenated solutions. Figure 5b shows that irradiation ($\lambda_{irr} \geq 395$ nm, 20 min) of 100 μM plasmid alone (5 mM Tris, pH = 7.5, 50 mM NaCl) does not result in photocleavage (lanes 1 and 2) and that the amount of photocleavage by 20 μM **2** (5 mM Tris, pH = 7.5, 50 mM NaCl) is similar when conducted in 50% D_2O (lane 5) compared to that in H_2O (lane 4) under similar conditions. Greater photocleavage would be expected in D_2O relative to H_2O if $^1O_2$ were involved in the reaction owing to its longer lifetime in the former.[94] Samples containing 100 μM plasmid and 20 μM **2** (5 mM Tris, pH = 7.5, 50 mM NaCl) bubbled with N_2 (lane 6) or subjected to five freeze−pump−thaw cycles (lane 7) resulted in slightly less photocleavage than those performed in air (lane 4), but a significant amount of photocleavage is apparent under deoxygenated conditions. These results indicate that oxygen plays some role in the observed DNA photocleavage of **1** and **2** but that an oxygen-independent pathway that results in cleavage is also operative. The DNA photocleavage by Rh(III) complexes possessing phi ligands has been previously shown to follow both oxygen-dependent and independent mechanisms.[95]

It should be noted that $Rh_2(O_2CCH_3)_4$ and $[Rh_2(O_2CCH_3)_2(phen)_2]^{2+}$ do not photocleave DNA directly but require an electron acceptor in solution for reactivity.[61,96] It is believed that photogenerated mixed-valent Rh(II,III) complex is the reactive species that effects DNA cleavage.[61] As shown in Figure 5, **1** and **2** are able to photocleave DNA directly, without an electron acceptor in solution.[96] Recent calculations

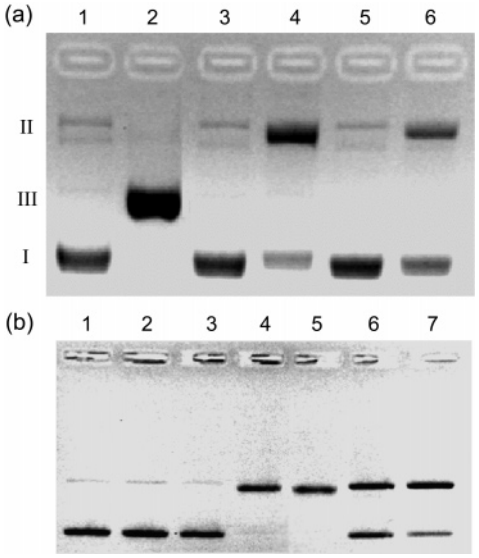

Figure 5. Ethidium bromide stained agarose gels (2%) of 100 μM pUC18 plasmid in the presence of 20 μM metal complex in 5 mM Tris, 50 mM NaCl (pH = 7.5) irradiated with $\lambda_{irr} > 395$ nm: (a) lane 1, plasmid only, dark; lane 2, plasmid + *Sma*I; lane 3, plasmid + **1**, dark; lane 4, plasmid + **1**, irr 15 min; lane 5, plasmid + **2**, dark; lane 6, plasmid + **2**, irr 15 min; (b) lane 1, plasmid only, dark; lane 2, plasmid only, irr 20 min; lane 3, plasmid + **2**, dark; lane 4, plasmid + **2**, irr 20 min, air; lane 5, plasmid + **2**, irr 20 min, 50% D_2O; lane 6, plasmid + **2**, irr 20 min, under N_2; lane 7, plasmid + **2**, irr 20 min, freeze−pump−thaw.

(90) Fu, P. K.-L., Bradley, P. M.; Turro, C. *Inorg. Chem.* **2003**, *42*, 878.
(91) Suh, D.; Oh, Y.-K.; Chaires, J. B. *Process Biochem.* **2001**, *37*, 521.
(92) Tang, T.-C.; Huang, H.-J. *Electroanalysis* **1999**, *11*, 1185.
(93) Paoletti, C.; Le Pecq, J. B.; Lehman, I. R. *J. Mol. Biol.* **1971**, *55*, 75.
(94) (a) Merkel, P. B.; Kearns, D. R. *J. Am. Chem. Soc.* **1972**, *94*, 1029. (b) Nekel, P. B.; Nilsson, R.; Kearns, D. R. *J. Am. Chem. Soc.* **1972**, *94*, 1030.
(95) Sitlani, A.; Long, E. C.; Pyle, A. M.; Barton, J. K. *J. Am. Chem. Soc.* **1992**, *114*, 2303.
(96) Bradley, P. M.; Angeles-Boza, A. M.; Dunbar, K. R.; Turro, C. *Inorg. Chem.* **2004**, *43*, 2450.

and experimental results concerning metal-to-ligand charge transfer (MLCT) excited states of Ru(II) and Re(I) dppz complexes may explain the difference in photoreactivity observed for **1** and **2** compared to $Rh_2(O_2CCH_3)_4$ and $[Rh_2(O_2CCH_3)_2(phen)_2]^{2+}$. Experiments and calculations have shown that the lowest lying excited states in $[Ru(bpy)_2(dppz)]^{2+}$ and *fac*-$[Re(CO)_3(dppz)(py)]^+$ are d(M) $\rightarrow \pi^*$(phz) MLCT in nature, where the transferred electron is localized in the phenazine (phz) part of the dppz ligand.[97,98] In both complexes this ^{3}MLCT state is nonemissive, and emission is observed from a triplet state in equilibrium with the d(M) $\rightarrow \pi^*$(phz) ^{3}MLCT.[97,98] A different ordering of states was later calculated for $[Ru(bpy)_2(dppz)]^{2+}$, but the lowest lying ^{3}MLCT state remained localized on the phenazine part of the dppz ligand.[99] Therefore, it is possible that, in **1** and **2**, a similar low-lying d(M) $\rightarrow \pi^*$(phz) ^{3}MLCT state is present. The spatial separation of the charge might render this excited state long lived, hence resulting in DNA cleavage by the oxidized dirhodium core. Time-resolved experiments and calculations are currently underway to elucidate the nature of the reactive excited state of **1** and **2**.

Cytotoxicity and Photocytotoxicity. The toxicity of **1** and **2** toward human skin cell (Hs-27) cultures was determined by measuring the percent survival in the presence of various amounts of complex relative to a control, which was not exposed to cytotoxic agents. Interpolation of the data points was used to determine the concentration of complex required to achieve 50% cell death, LC_{50} (LC = lethal concentration). The photocytotoxicity of **1** and **2** were determined from measurements of LC_{50} values for Hs-27 cell cultures exposed to 400−700 nm light for 30 min (5 J/cm^2). Plots of percent Hs-27 survival as a function of increasing concentrations of **1** and **2** in the dark and irradiated with visible light are shown in Figure 6. The LC_{50} values determined for **1** are similar for cultures in the dark (30 min exposure) and upon irradiation, 27 ± 2 and 21 ± 3 μM, respectively. In contrast, a much higher LC_{50} was measured for **2** in the dark (135 ± 8 μM) indicative of significantly lower cytotoxicity. Upon irradiation with visible light, the cytotoxicity of **2** increases significantly, resulting in $LC_{50} = 39 \pm 1$ μM. It should be noted that the LC_{50} value measured for **2** in the dark is comparable to that of cisplatin (131 ± 10 μM) for Hs-27 cells under similar experimental conditions in the dark. As expected, irradiation with visible light has little effect on the cytotoxicity of cisplatin, $LC_{50} = 110 \pm 10$ μM. It should be noted that the LC_{50} value measured for cisplatin in this study is higher than previously reported values, but the difference can be explained by the shorter incubation times and the differences in toxicity of the complex as a function of cell line. The shorter time for exposure of the cells to the compounds is based on the fact that the irradiation studies were performed for 30 min. Exposure of cisplatin to Hs-27 for 8, 16, and 24 h results in LC_{50} values of 8.6 ± 0.5, 4.4 ± 0.3, and 4.5 ± 0.3 μM, respectively. For comparison, we note that the LC_{50} values reported for 24 h exposure to cisplatin of human epidermal cells, human uterus cancer cells (HeLa), and human leukemia cells (U-937) are <4, 8, and 50 μM, respectively.[100,101] In a different study, 24 h exposure of cisplatin to HeLa cells resulted in $LC_{50} = 0.50 \pm 0.05$ μM,[102] and human colon cancer cells in contact with cisplatin for 2 h yielded an LC_{50} value of 26 μM.[103] In addition, the LC_{50} values recently reported for a variety of cell lines for cisplatin range from 7 to 164 μM (24 h).[104]

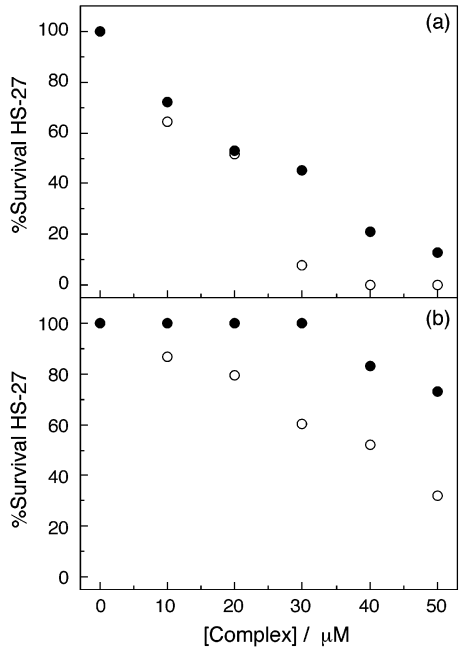

Figure 6. Plot of percent survival of human skin cells (Hs-27) as a function of concentration of (a) **1** and (b) **2** in the dark (●) and irradiated with 400−700 nm light for 30 min (○).

The cytotoxic effect of **1** in the dark is not unexpected given its ability to intercalate DNA and shift the DNA melting temperature by 21 °C. These features may disrupt crucial cellular functions, such as transcription and DNA replication. Irradiation of Hs-27 cultures exposed to **1** with visible light does not appear to result in significant additional cell death, although the DNA photocleavage by **1** is greater than that observed for **2** (Figure 5a). In contrast, the LC_{50} of **2** decreases upon photolysis. For example, Figure 6 shows 100% survival of Hs-27 cells exposed to 30 μM **2** in the dark, but the same concentration of **2** results in ~40% cell death when the culture is irradiated with visible light. The inability of **2** to intercalate the DNA base π-stack may

(97) Brennaman, M. K.; Alstrum-Acevedo, J. H.; Fleming, C. N.; Jang, P.; Meyer, T. J.; Papanikolas, J. M. *J. Am. Chem. Soc.* **2002**, *124*, 15094.
(98) Dyer, J.; Blau, W. J.; Coates, C. G.; Creely, C. M.; Gavey, J. D.; George, M. W.; Grills, D. C.; Hudson, S.; Kelly, J. M.; Matousek, P.; McGarvey, J. J.; McMaster, J.; Parker, A. W.; Towrie, M.; Weinstein, J. A. *Photochem. Photobiol. Sci.* **2003**, *2*, 542.
(99) Pourtois, G.; Belijonne, D.; Moucheron, C.; Schumm, S.; Kirsh-De Mesmaeker, A.; Lazzaroni, R.; Brédas, J.-L. *J. Am. Chem. Soc.* **2004**, *126*, 683.
(100) Featherstone, J.; Dykes, P. J.; Marks, R. *Skin Pharmacol.* **1991**, *4*, 169.
(101) Cervantes, G.; Marchal, S.; Prieto, M. J.; Pérez, J. M.; González, V. M.; Alonso, C.; Moreno, V. *J. Inorg. Biochem.* **1999**, *77*, 197.
(102) Sandman, K. E.; Fuhrman, P.; Lippard, S. J. *J. Biol. Inorg. Chem.* **1998**, *3*, 74.
(103) Gharehbaghi, K.; Szekeres, T.; Yalowitz, J. A.; Fritzer-Szekeres, M.; Pommier, Y. G.; Jayaram, H. N. *Life Sci.* **2000**, *68*, 1.
(104) Gómez Quiroga, A.; Navarro Ranninger, C. *Coord. Chem. Rev.* **2004**, *248*, 119.

account for its low LC_{50} value in the dark relative to that measured for **1**. However, additional factors besides intercalation are likely to play a role in the cytotoxicity of dirhodium complexes, since the LC_{50} values for the nonintercalating complex $Rh_2(O_2CCH_3)_4$ ($K_b = 4.6 \times 10^2\ M^{-1}$)[60] are 15 ± 2 and $13 \pm 2\ \mu M$ in the dark and irradiated, respectively. The low toxicity of **2** in the dark and its increase upon irradiation are desirables features for a potential photochemotherapy agent, where an otherwise nontoxic compound becomes lethal upon exposure to low-energy visible light.

Conclusions

Two new dirhodium(II) complexes possessing the intercalating dppz ligand, *cis*-$[Rh_2(\mu\text{-}O_2CCH_3)_2(dppz)(\eta^1\text{-}O_2CCH_3)(CH_3OH)]^+$ (**1**) and *cis*-$[Rh_2(\mu\text{-}O_2CCH_3)_2(dppz)_2]^{2+}$ (**2**), were synthesized and characterized as potential complexes for photochemotherapy. Various techniques support the conclusion that **1** binds to DNA through intercalation, although some aggregation of the complex on the DNA surface is also present. In contrast, compound **2** does not intercalate between the DNA bases, and the strong hypochromic behavior observed in the presence of DNA is attributed to intermolecular π-stacking of **2** enhanced by the polyanion. The apparent DNA binding constants determined using optical titrations were compared to those from dialysis experiments. Both complexes photocleave pUC18 plasmid in vitro under irradiation with visible light ($\lambda_{irr} \geq 395$ nm, 15−20 min), resulting in the nicked, circular form. Greater photocleavage is observed for **1** compared to **2**, which may be explained by the ability of **1** to intercalate. The cytotoxicity of **2** toward human skin cells ($LC_{50} = 135 \pm 8\ \mu M$) is significantly lower than those of **1** ($LC_{50} = 27 \pm 2\ \mu M$) and $Rh_2(O_2CCH_3)_4$ ($LC_{50} = 15 \pm 2\ \mu M$). Irradiation of cell cultures containing **1** and $Rh_2(O_2CCH_3)_4$ with visible light has little effect on their cytotoxicity, with LC_{50} values of 21 ± 3 and $13 \pm 2\ \mu M$, respectively. In contrast, the toxicity of **2** increases significantly when the cell cultures are irradiated with visible light (400−700 nm, 30 min), resulting in $LC_{50} = 39 \pm 1\ \mu M$. This difference in cytotoxicity in the dark and upon photolysis makes **2** a potential candidate for photochemotherapy. It should be noted that although **1** is able to induce greater DNA photocleavage in vitro than **2**, its cytotoxicity properties do not make **1** a good candidate for photochemotherapy. The ability of **1** to intercalate between the DNA bases likely renders this complex too cytotoxic in the dark, which suggests that intercalation may not be a desired property of a successful photochemotherapy agent.

Acknowledgment. K.R.D. thanks Johnson-Matthey for a generous gift of $Rh_2(\mu\text{-}O_2CCH_3)_4$. C.T. thanks the National Institutes of Health (Grant RO1 GM64040-01) for their generous support. K.R.D. thanks the State of Texas for an ARP grant (010366-0277-1999) and the Welch Foundation (A1449) for financial support.

Supporting Information Available: Additional crystal structure data. This material is available free of charge via the Internet at http://pubs.acs.org.

IC049091H